Evaluation and design of linear reconstruction methods with the frequency error kernel

Laurent Condat

CNRS research fellow at GIPSA-lab, Grenoble, France

2012

Motivation

$s(\mathbf{x})$

↓

$s(\mathbf{x}/3)$

↓

…

scene

$s(\mathbf{x}), \quad \mathbf{x} \in \mathbb{R}^2$

acquisition

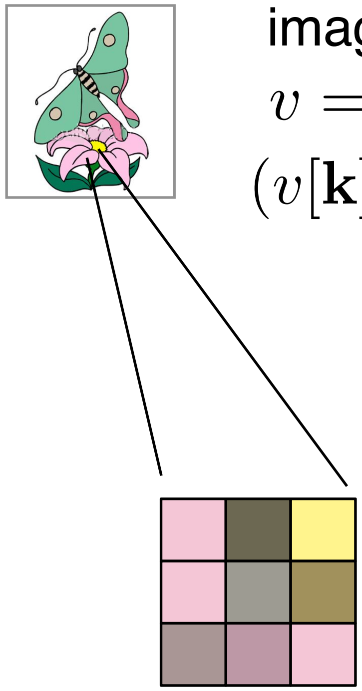

image

$v = (v[\mathbf{k}])_{\mathbf{k}\in\mathbb{Z}^2}$

continuous functions: operations well-posed

operations on discrete signals/ images?

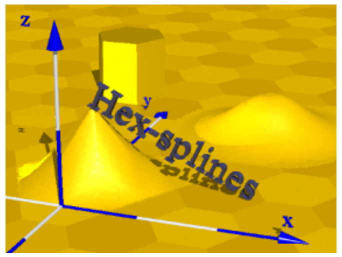

Reconstruction: an inverse problem

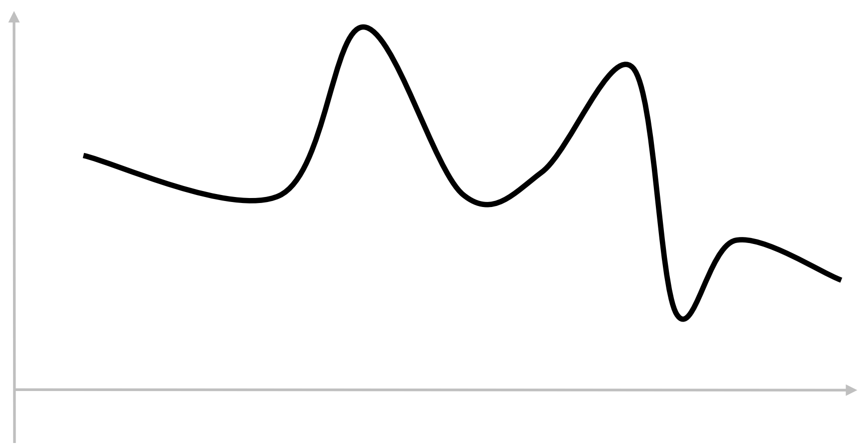

acquisition →

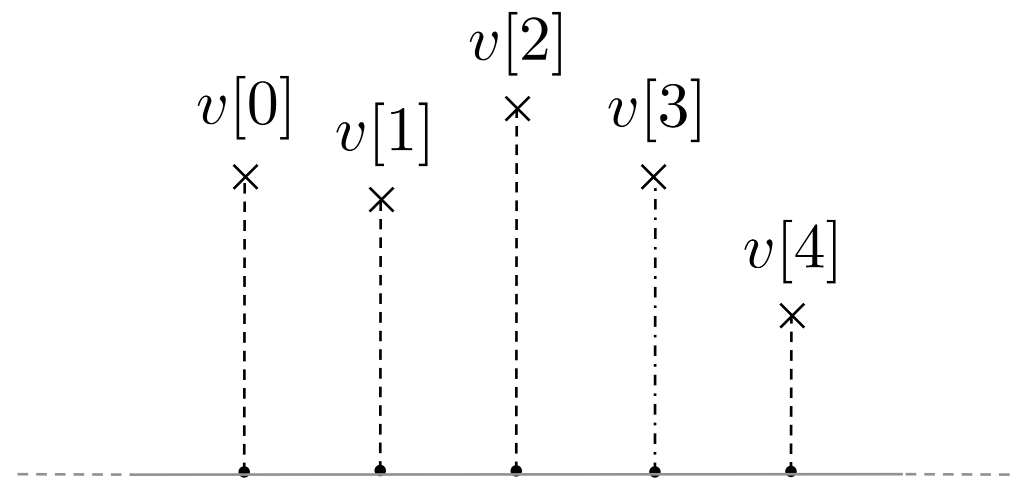

process $s(t),\ t \in \mathbb{R}$

samples $v[k],\ k \in \mathbb{Z}$

$$f_{\text{app}} \approx s \xleftarrow{\textbf{reconstruction}} v$$

: ill-posed inverse problem

acquisition model:

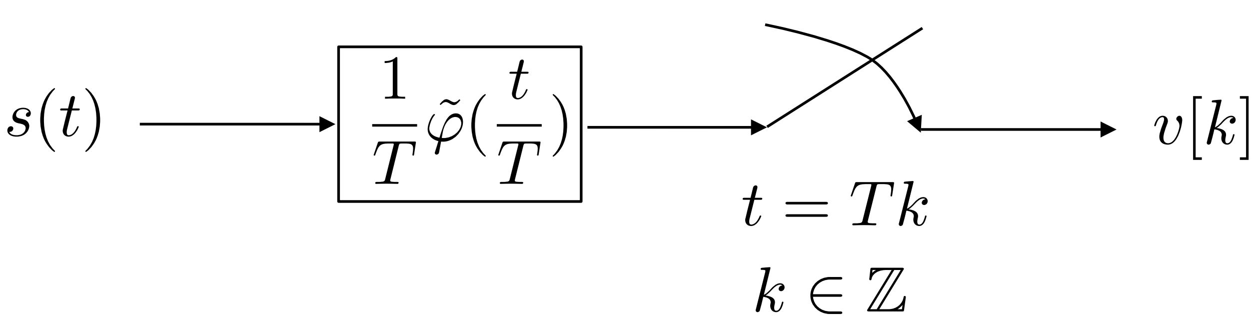

$s(t)$: unknown function

$\tilde{\varphi}(t)$: impulse response

T : sampling step

Some classical reconstruction frameworks

- Stochastic framework: minimize $\mathcal{E}\{|s(t) - f_{\text{app}}(t)|^2\} \quad \forall t \in \mathbb{R}$ [Unser, Ramani]

  → Wiener-like solution; depends on the power spectrum density of s

- Variational framework: minimize the regularized least-squares criterion

$f_{\text{app}} = \underset{g \in L_2}{\text{argmin}} \sum_{k \in \mathbb{Z}} |\mathcal{D}g[k] - v[k]|^2 + \lambda \|\mathcal{L}g\|_{L_2}^2$ for some functional $\mathcal{L}$, e.g. $\mathcal{L}\cdot = \frac{d^n \cdot}{dt^n}$

- Minimax framework: minimize the worst-case L_2-error in some quadratic set.

$\Omega = \{g \in L_2 \ ; \ \|\mathcal{L}g\|^2 \leq C\}$ [Eldar, Dvorkind]

LSI reconstruction spaces

- Common point in all classical settings:
  f_{app} belongs to some linear shift-invariant (LSI) functional space

$$f_{\mathrm{app}} \in V_T(\varphi) = \left\{ \sum_{k\in\mathbb{Z}} c[k]\varphi(\frac{t}{T} - k) \ ; \ c \in \mathbb{R}^{\mathbb{Z}} \right\}$$ for some generator $\varphi(t)$

- « think analog, act digital » [Unser] : f_{app} has a parametric form

$$f_{\mathrm{app}}(t) = \sum_{k\in\mathbb{Z}} c[k]\varphi(\frac{t}{T} - k)$$ with $$c = v * p$$

LSI reconstruction spaces

- Common point in all classical settings:
  f_{app} belongs to some linear shift-invariant (LSI) functional space

$$f_{\text{app}} \in V_T(\varphi) = \left\{ \sum_{k\in\mathbb{Z}} c[k]\varphi(\frac{t}{T} - k) \ ; \ c \in \mathbb{R}^{\mathbb{Z}} \right\}$$ for some generator $\varphi(t)$

- The best L_2-reconstruction of s is $\mathcal{P}_T s$

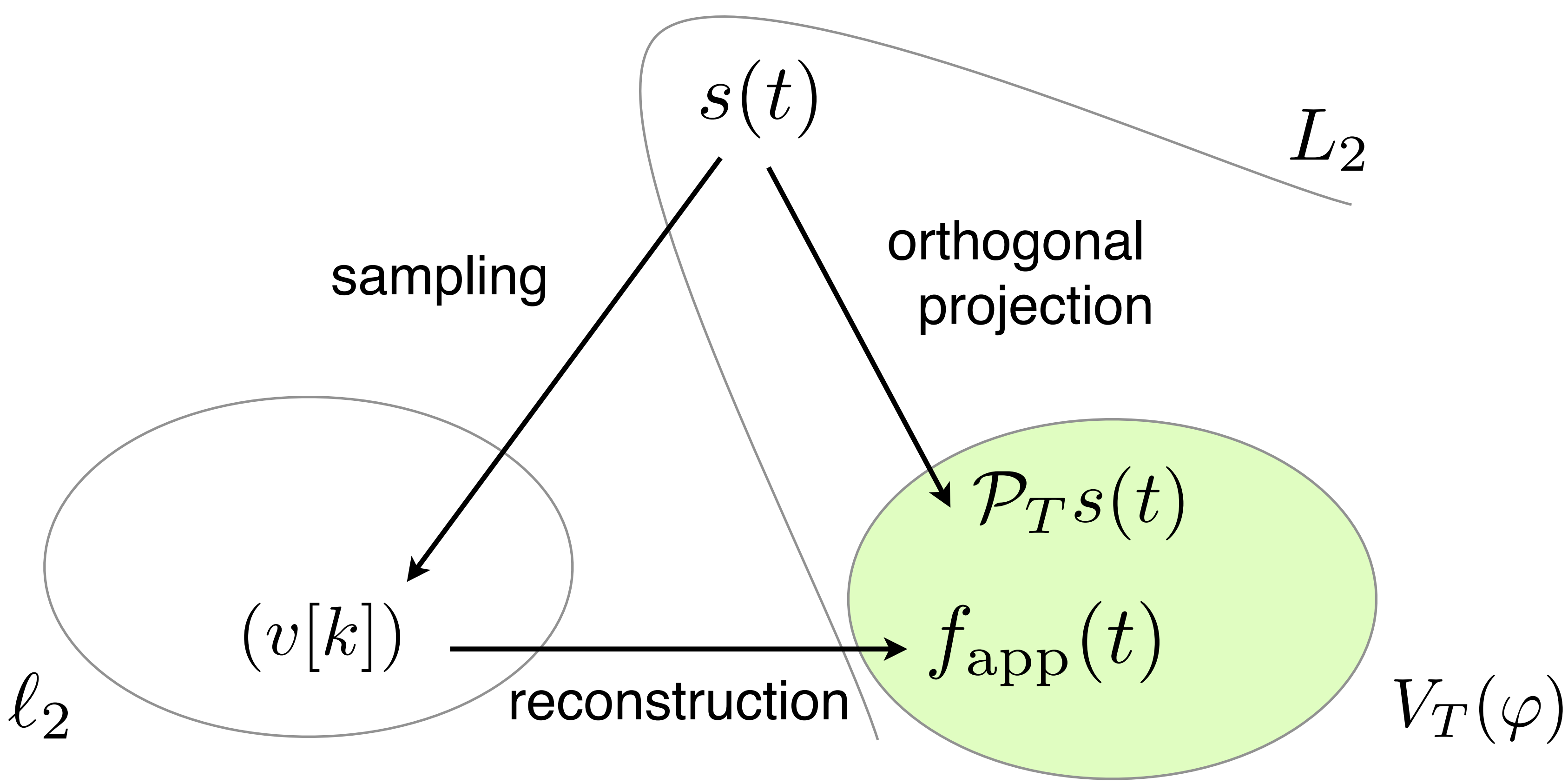

The frequency error kernel

- Result of approximation theory [Blu et al., 99]:

$$\|s - f_{\text{app}}\|_{L_2}^2 \approx \frac{1}{2\pi}\int_{\mathbb{R}} |\hat{s}(\omega)|^2 E(T\omega)d\omega$$

where $E(\omega)$ is the frequency error kernel:

$$E(\omega) = 1 - \frac{|\hat{\varphi}(\omega)|^2}{\hat{a}_\varphi(\omega)} + \hat{a}_\varphi(\omega)\left|\hat{p}(\omega)\hat{\tilde{\varphi}}(\omega) - \frac{\hat{\varphi}(\omega)^*}{\hat{a}_\varphi(\omega)}\right|^2$$

($\hat{a}_\varphi(\omega) = \sum_{\mathbb{Z}} |\hat{\varphi}(\omega + 2k\pi)|^2$)

- stochastic framework:

$$\frac{1}{T}\int_0^T \mathcal{E}\{|s(t) - f_{\text{app}}(t)|^2\}dt = \frac{1}{2\pi}\int_{\mathbb{R}} \hat{c}_s(\omega)E(T\omega)d\omega$$

The frequency error kernel

- Result of approximation theory [Blu et al., 99]:

$$\|s - f_{\text{app}}\|_{L_2}^2 \approx \frac{1}{2\pi} \int_{\mathbb{R}} |\hat{s}(\omega)|^2 E(T\omega) d\omega$$

where $E(\omega)$ is the frequency error kernel:

$$E(\omega) = 1 - \frac{|\hat{\varphi}(\omega)|^2}{\hat{a}_\varphi(\omega)} + \hat{a}_\varphi(\omega) \left| \hat{p}(\omega)\hat{\tilde{\varphi}}(\omega) - \frac{\hat{\varphi}(\omega)^*}{\hat{a}_\varphi(\omega)} \right|^2$$

The approximation $\approx$ is exact in many cases, e.g. for bandlimited functions or when averaging over the shifts of s

Frequency error kernel: properties

$$E(\omega) = 1 - \frac{|\hat{\varphi}(\omega)|^2}{\hat{a}_\varphi(\omega)} + \hat{a}_\varphi(\omega)\left|\hat{p}(\omega)\hat{\tilde{\varphi}}(\omega) - \frac{\hat{\varphi}(\omega)^*}{\hat{a}_\varphi(\omega)}\right|^2$$

$E(\omega)$ is the relative error at the frequency ω :
it describes the time-averaged error when $s(t) = \sin(\omega T)$

The behavior of $E(\omega)$ around $\omega = 0$ characterizes the error for the low-frequency part of s

Asymptotic result: if s is smooth enough (Sobolev sense),

$$\|f_{\text{app}} - s\|_{L_2} \sim C\|s^{(L)}\|_{L_2} T^L \;\Leftrightarrow\; \sqrt{E(\omega)} \sim C\omega^L$$

Designing reconstruction schemes

- Strategy: minimizing C in $\sqrt{E(\omega)} \sim C\omega^L$ among a class of functions, e.g. the cubic MOMS

[Blu *et al.*, IEEE TIP, 01]

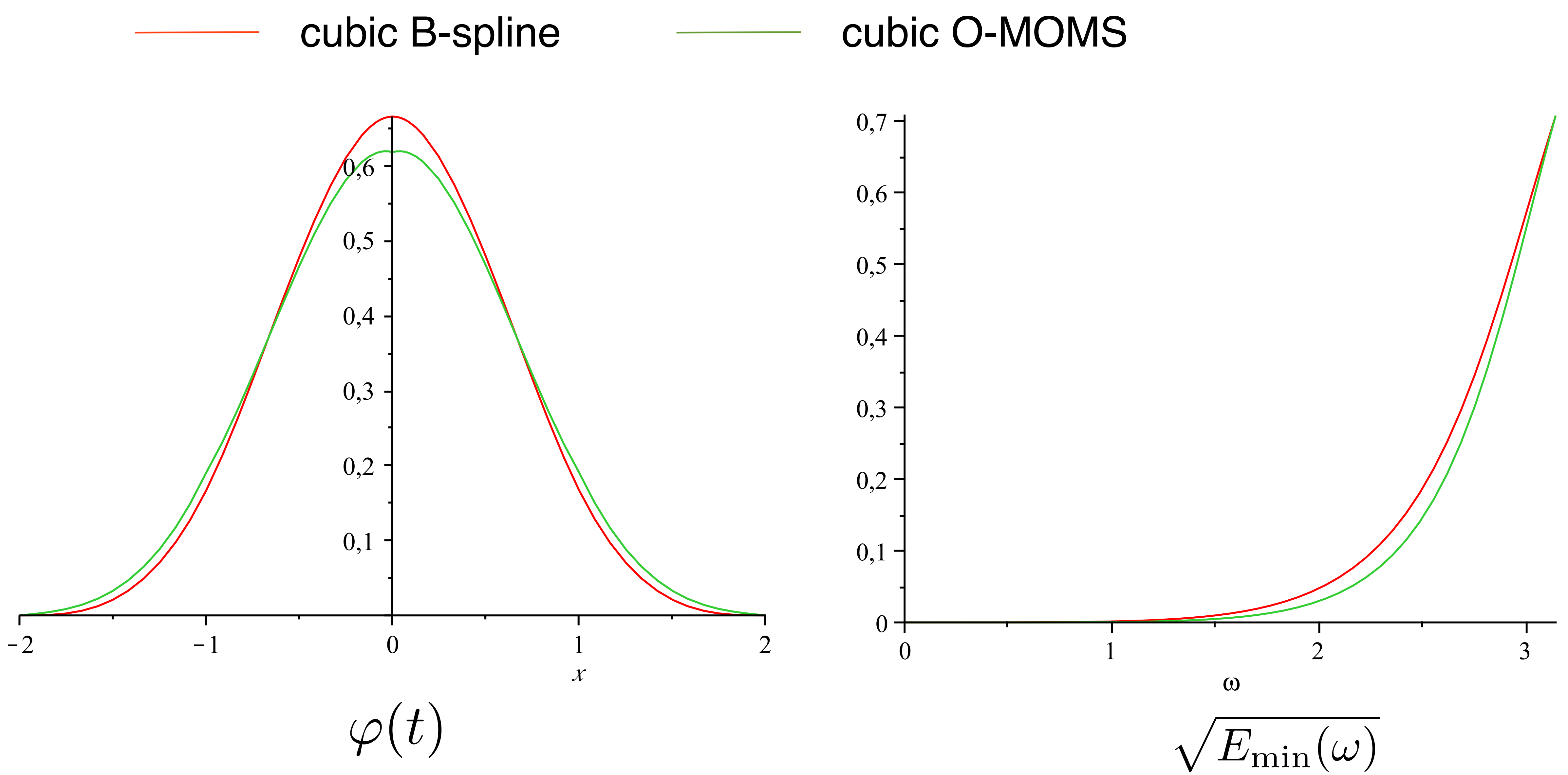

Consistent reconstruction

Once the LSI reconstruction space $V_T(\varphi)$ is fixed:
the usual solution is to choose the unique function in $V_T(\varphi)$
which is consistent with the data, i.e. $\mathcal{D}f_{\text{app}} = v$

$$s \overset{\mathcal{D}}{\mapsto} (v[k])$$

- → f_{app} is the oblic projection of s in $V_T(\varphi)$
- → can be quite different from the orthogonal projection:

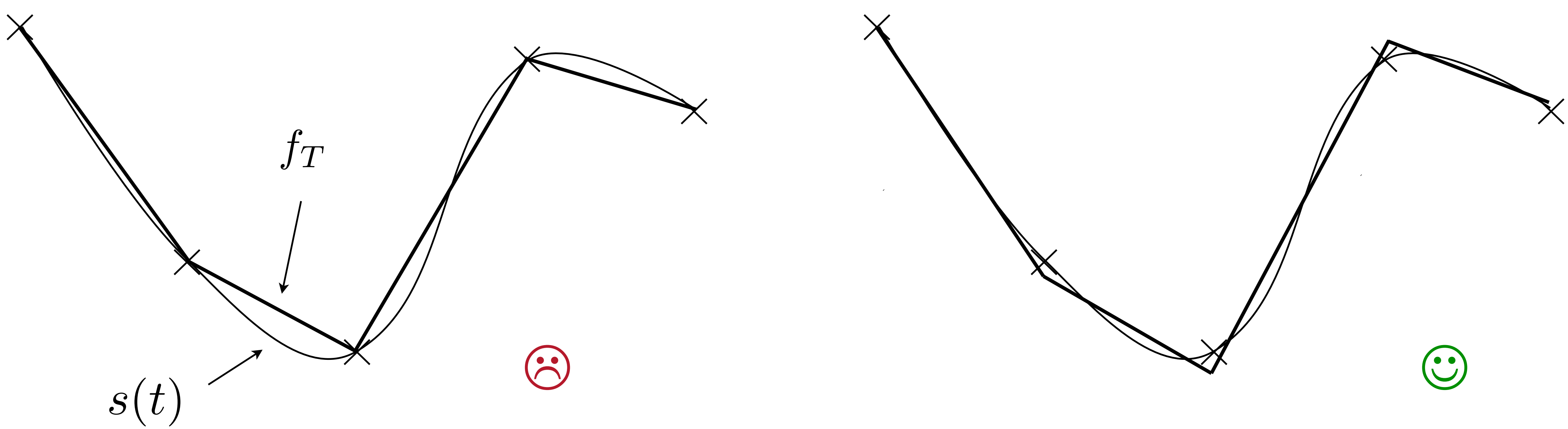

Designing reconstruction schemes

- When φ is fixed, choose p so that $E(\omega) \sim E_{\min}(\omega) \sim C^2_{\min}\omega^{2L}$

  → amounts to performing a quasi-projection of s in $V_T(\varphi)$

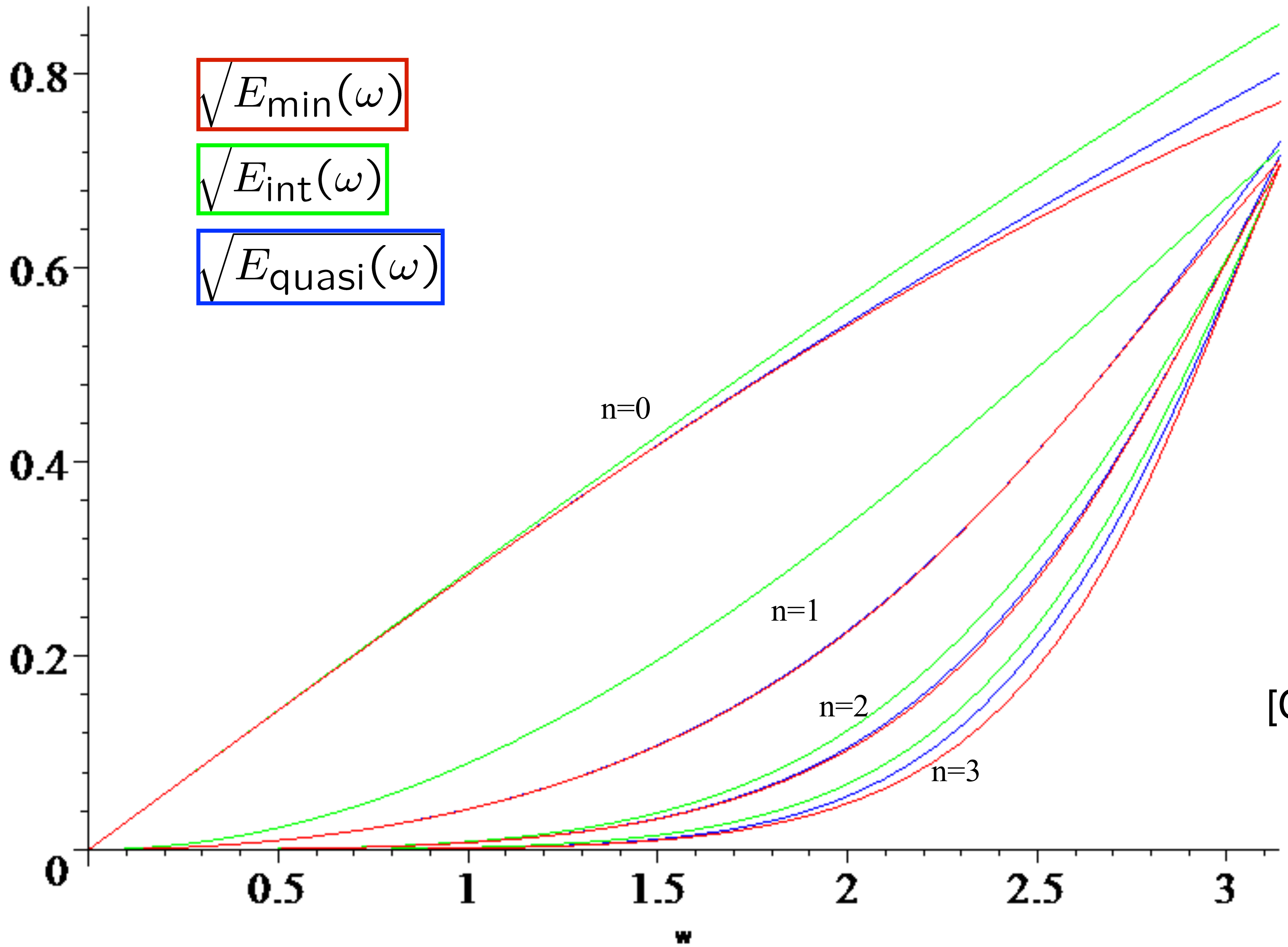

example: spline optimal quasi-interpolation with inverse prefilters

[Condat, Blu, Unser, ICIP 05]

Validation: successive rotations of angle $2\pi/7$

initial image | bilinear interpolation **1** | bilinear quasi-int.

Validation: successive rotations of angle $2\pi/7$

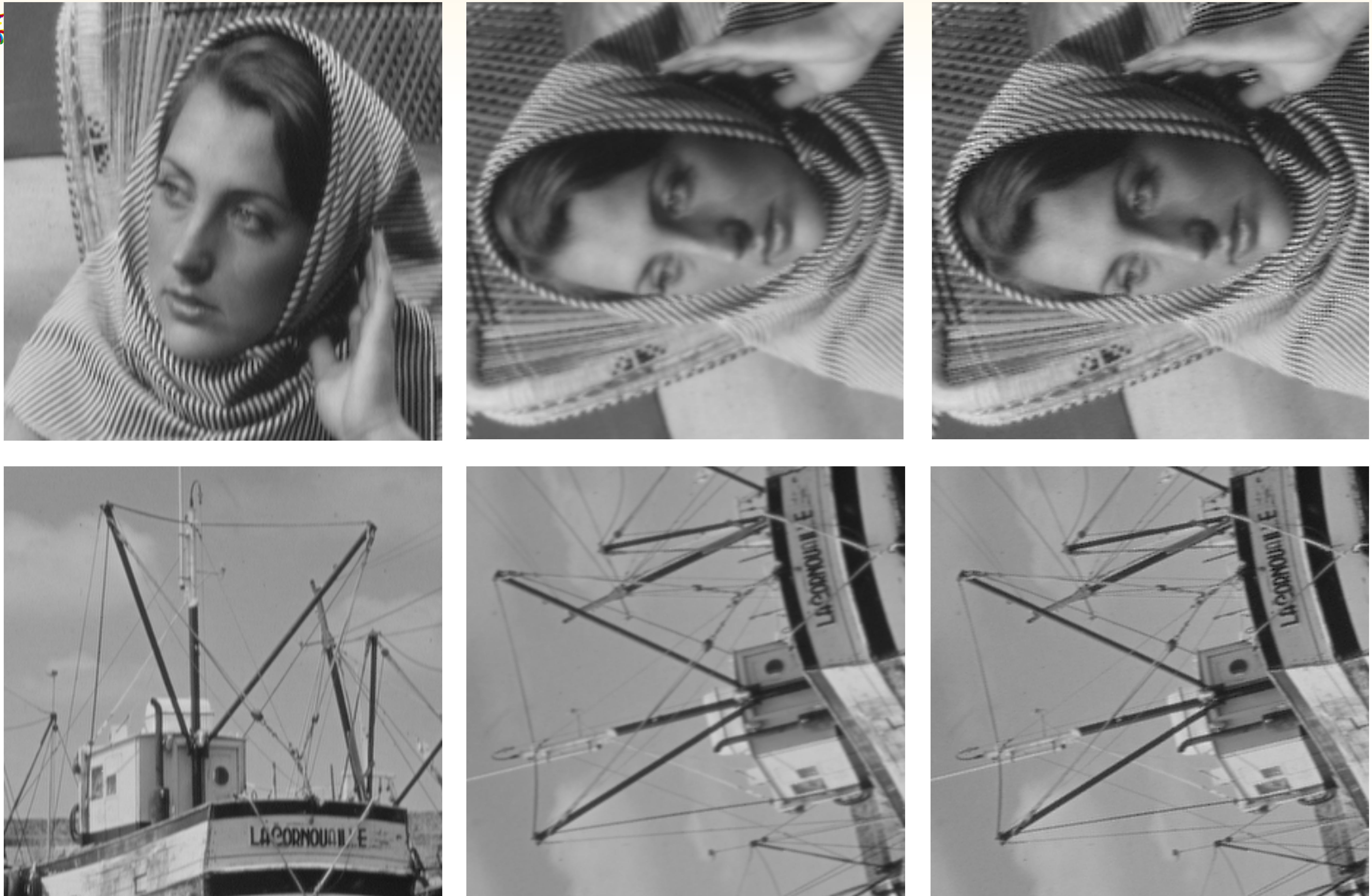

initial image | bilinear interpolation **2** | bilinear quasi-int.

Validation: successive rotations of angle $2\pi/7$

initial image | bilinear interpolation | **3** | bilinear quasi-int.

Validation: successive rotations of angle $2\pi/7$

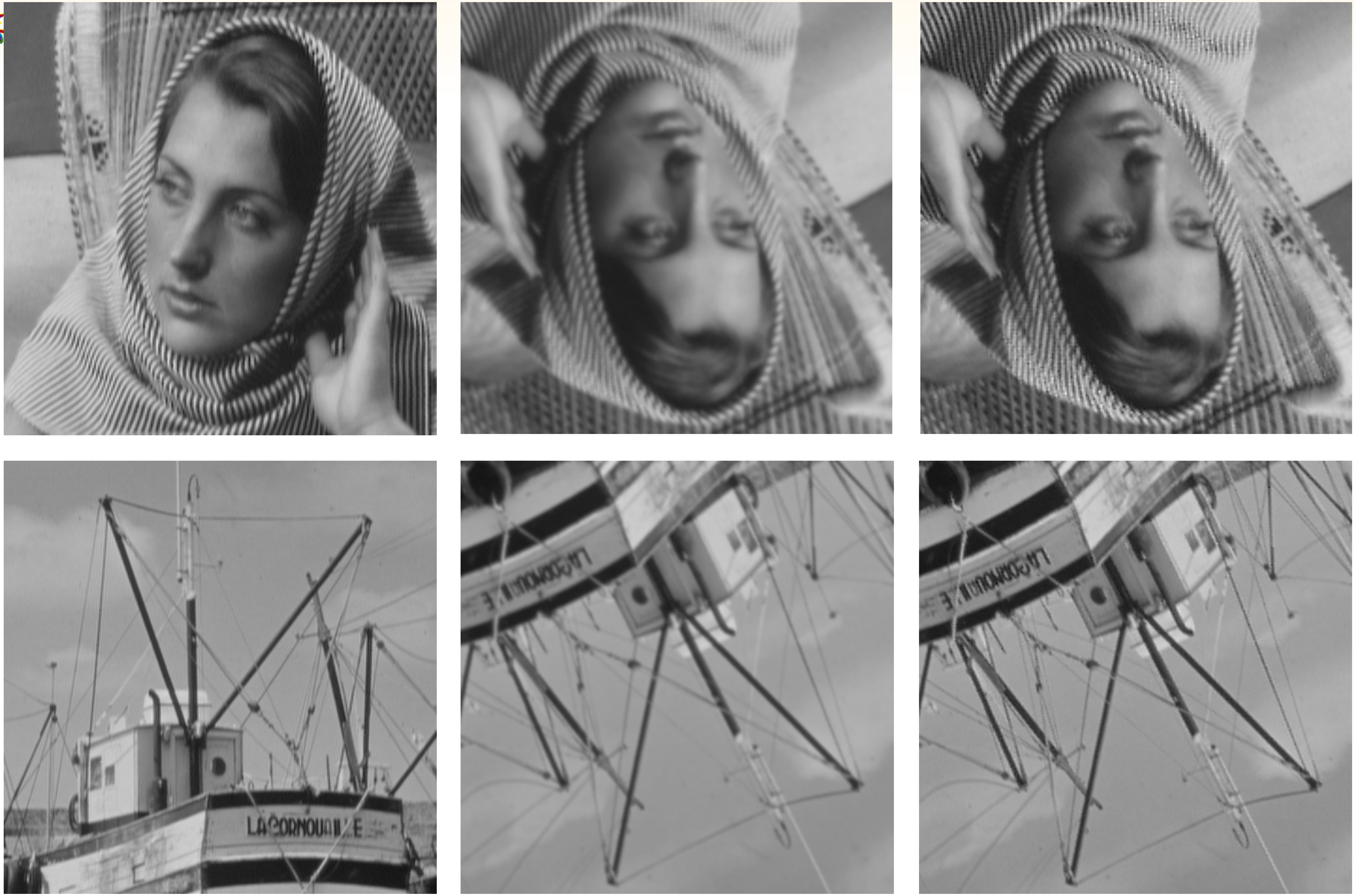

initial image bilinear interpolation **4** bilinear quasi-int.

Validation: successive rotations of angle $2\pi/7$

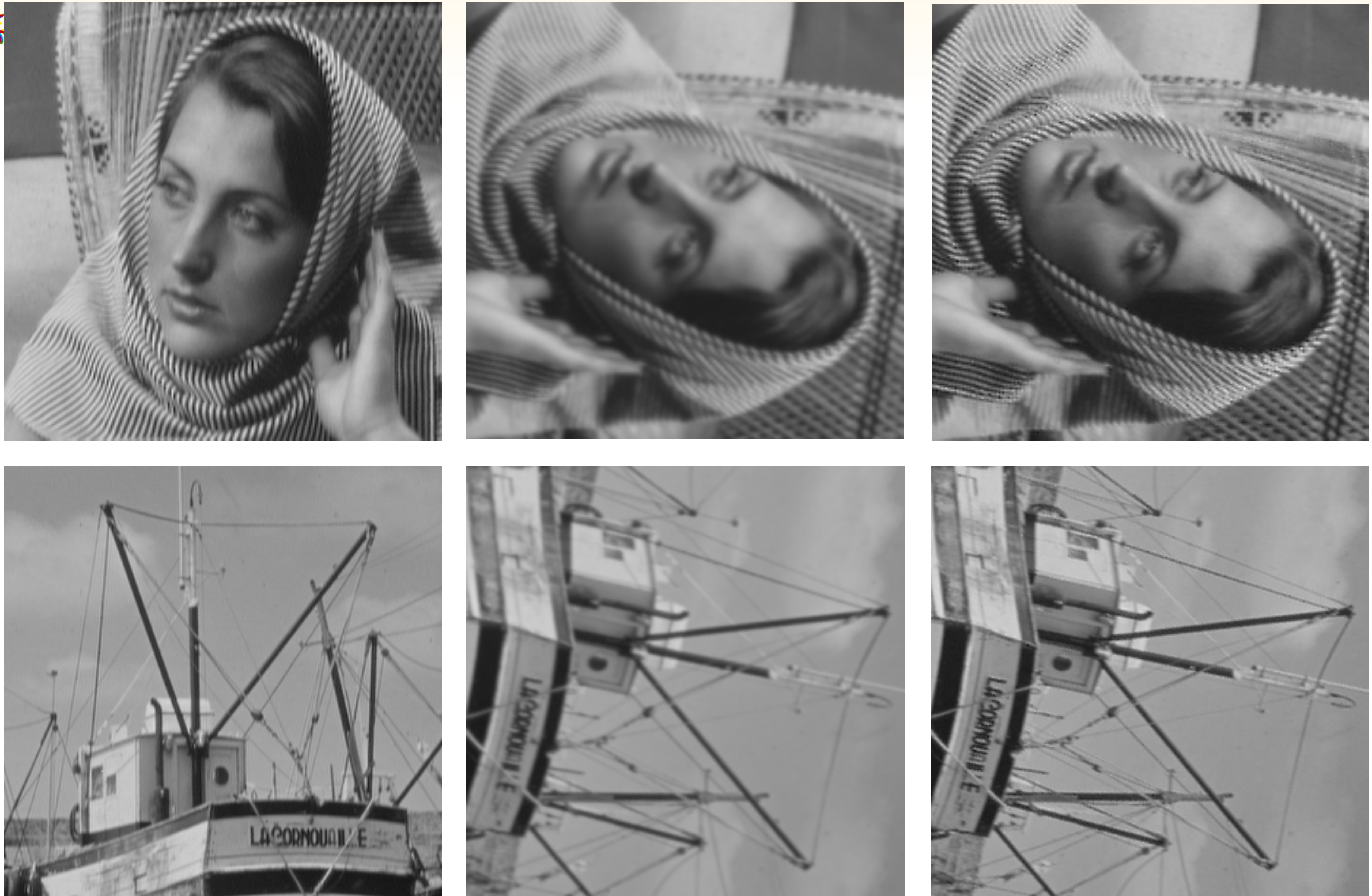

initial image | bilinear interpolation **5** | bilinear quasi-int.

Validation: successive rotations of angle $2\pi/7$

initial image | bilinear interpolation | **6** | bilinear quasi-int.

Validation: successive rotations of angle $2\pi/7$

initial image | bilinear interpolation **7** | bilinear quasi-int.

Multi-D case: signals on lattices

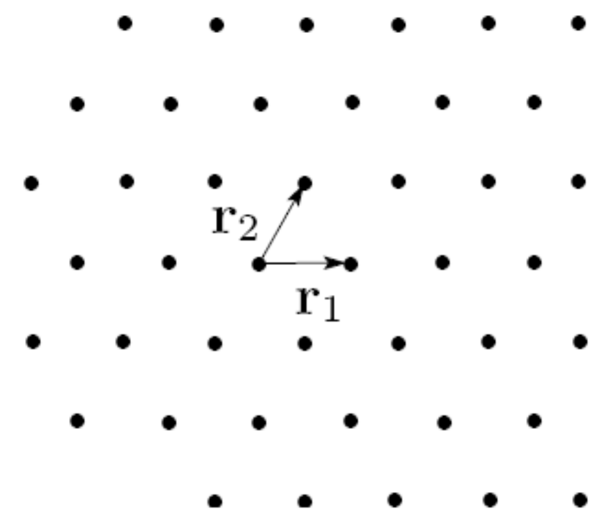

The hexagonal lattice

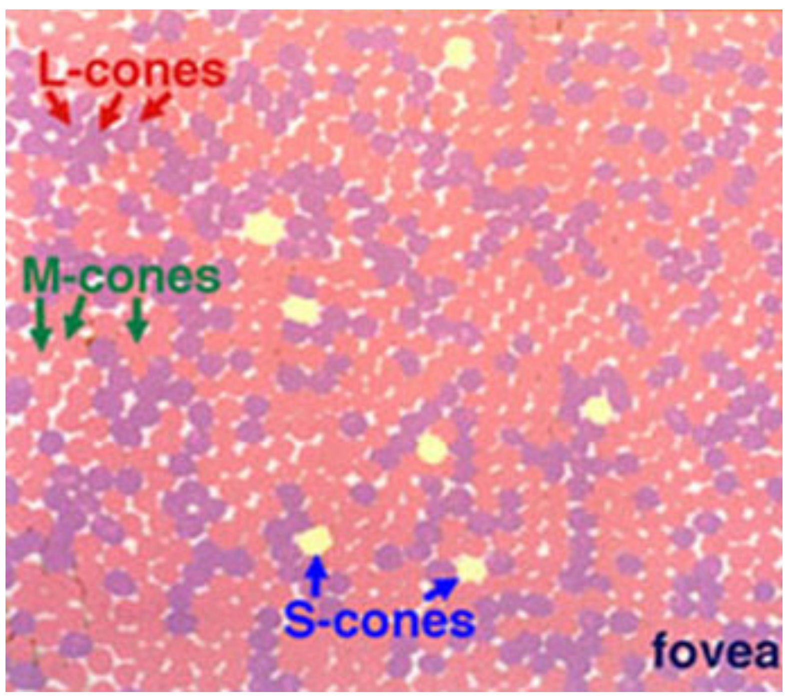

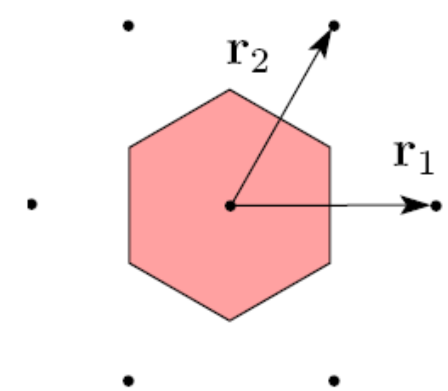

- There exist sensors with hex. geometry, e.g. in mammography [Laine'93]

Reconstruction on the hex. lattice

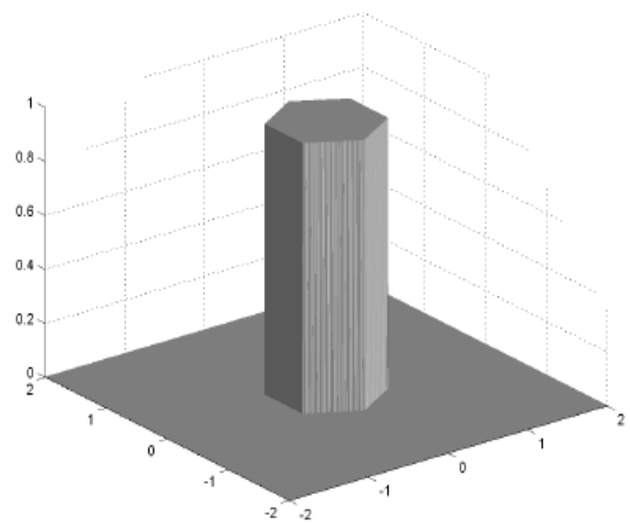
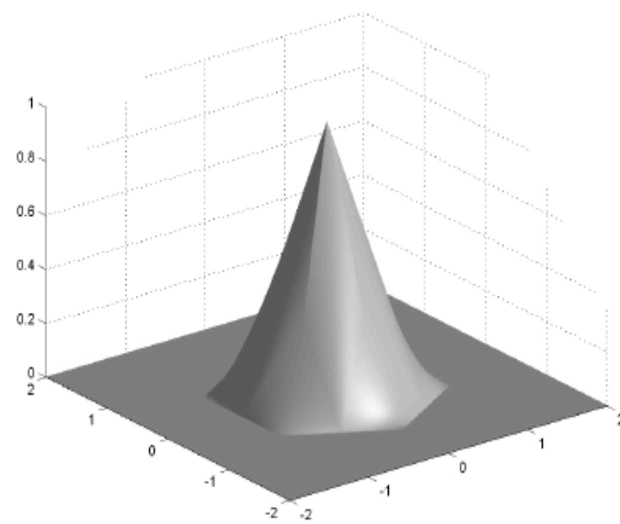
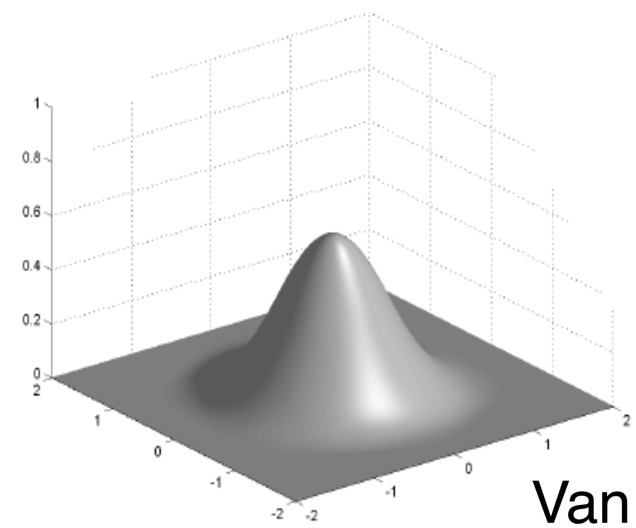

hex-splines

Van De Ville *et al.*, TIP 06

Condat, Van De Ville, TIP 07

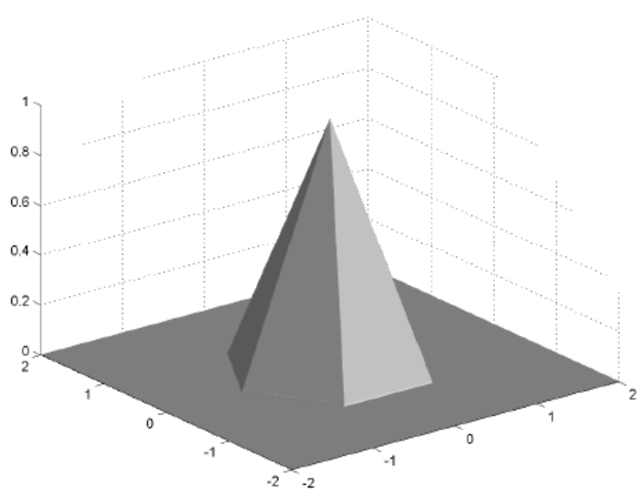
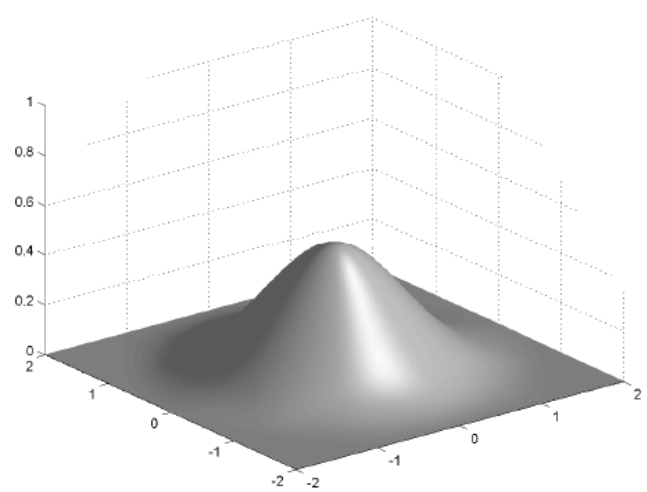

box-splines:
new characterization +
fast implementation

Condat, Van De Ville, SPL 06

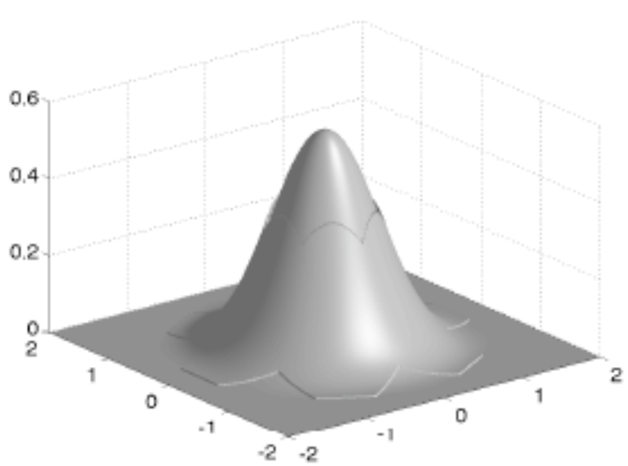
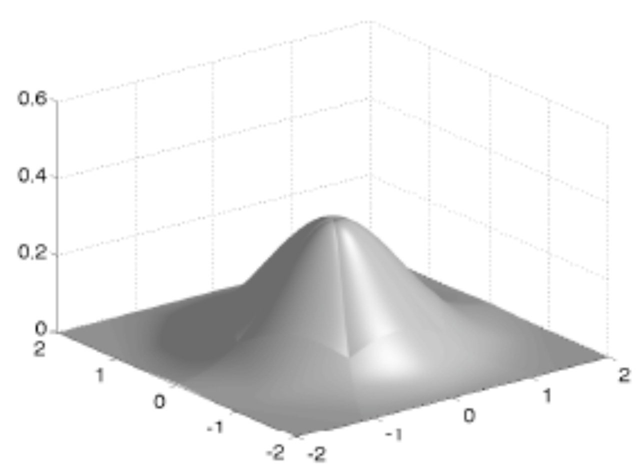

“hex-MOMS”

Condat, Van De Ville, ICIP 08

Comparison of 2D lattices

- Examples of kernels $E_{\min}(\boldsymbol{\omega})$

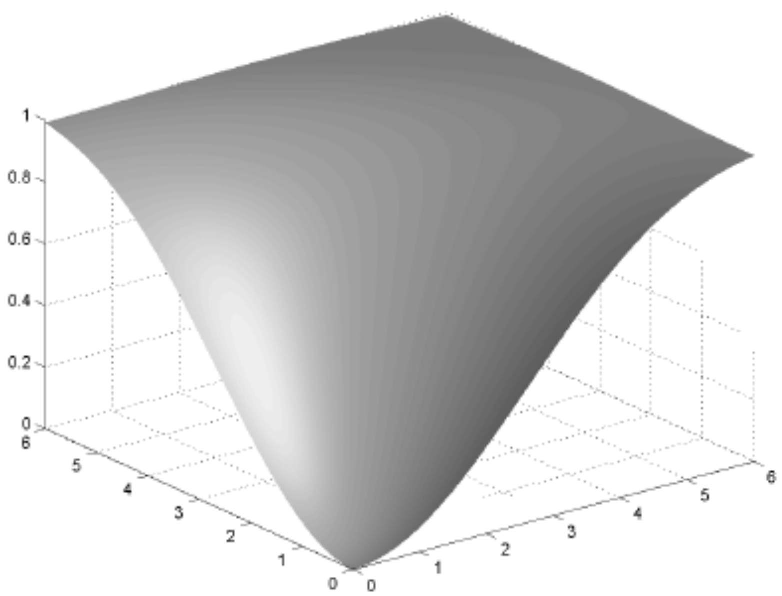

$\varphi = \eta_1$

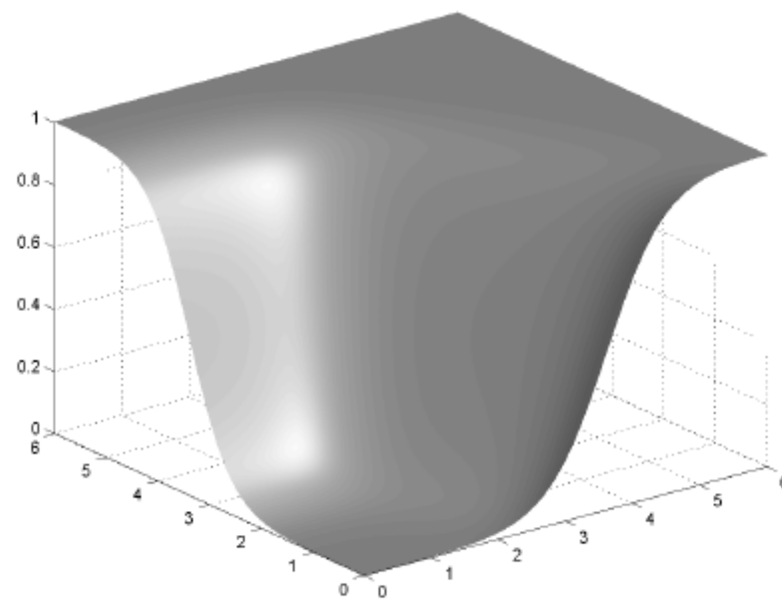

$\varphi = \eta_2$

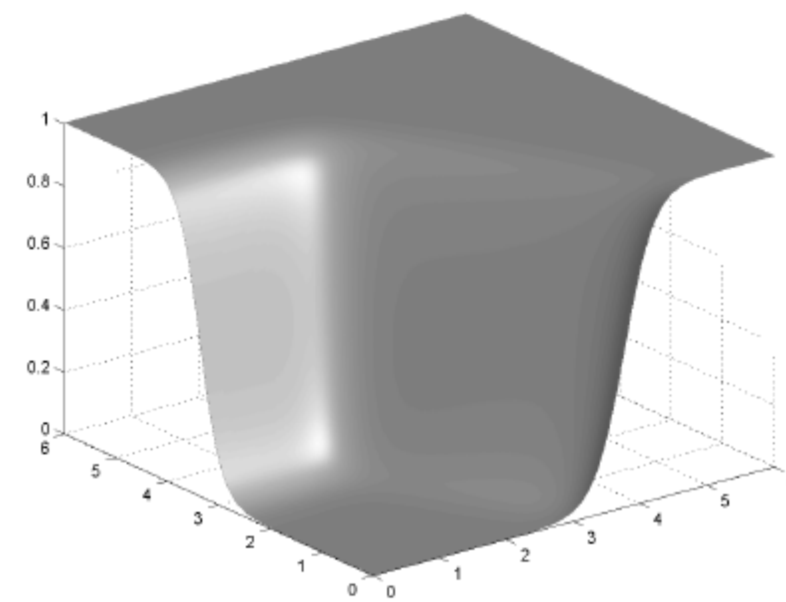

$\varphi = \chi_4$

- Asymptotic behavior: $E(\boldsymbol{\omega}) \sim C(\theta)\|\boldsymbol{\omega}\|^{2L}$
- Comparison of the constants C: asymptotically, the same reconstruction quality is obtained on a hexagonal lattice with 40% less samples than on a Cartesian lattice.

[Condat, Van De Ville, Blu, ICIP 2005]

[Condat, Möller, IEEE TSP 2011]

Reconstruction of derivatives

- New result: $$\|s^{(N)} - f_{\mathrm{der}}\|_{L_2}^2 \approx \frac{1}{2\pi}\int_{\mathbb{R}} \underbrace{|\hat{s}(\omega)|^2 \omega^{2N}}_{|\widehat{s^{(N)}}(\omega)|^2} E(T\omega)d\omega$$

  where $E(\omega)$ is the frequency error kernel:

$$E(\omega) = 1 - \frac{|\hat{\varphi}(\omega)|^2}{\hat{a}_\varphi(\omega)} + \hat{a}_\varphi(\omega)\left|\hat{p}(\omega)\hat{\tilde{\varphi}}(\omega)\frac{1}{(j\omega)^N} - \frac{\hat{\varphi}(\omega)^*}{\hat{a}_\varphi(\omega)}\right|^2$$

- Stochastic framework:

$$\frac{1}{T}\int_0^T \mathcal{E}\{|s^{(N)}(t) - f_{\mathrm{der}}(t)|^2\}dt = \frac{1}{2\pi}\int_{\mathbb{R}} \hat{c}_s(\omega)\omega^{2N}E(T\omega)d\omega$$

Reconstruction error: example

Reconstruction of $s'(t)$ where $s(t) = e^{-\frac{(t-1)^2}{2}}$ by the derivative of the cubic spline interpolant.

$s(t)$

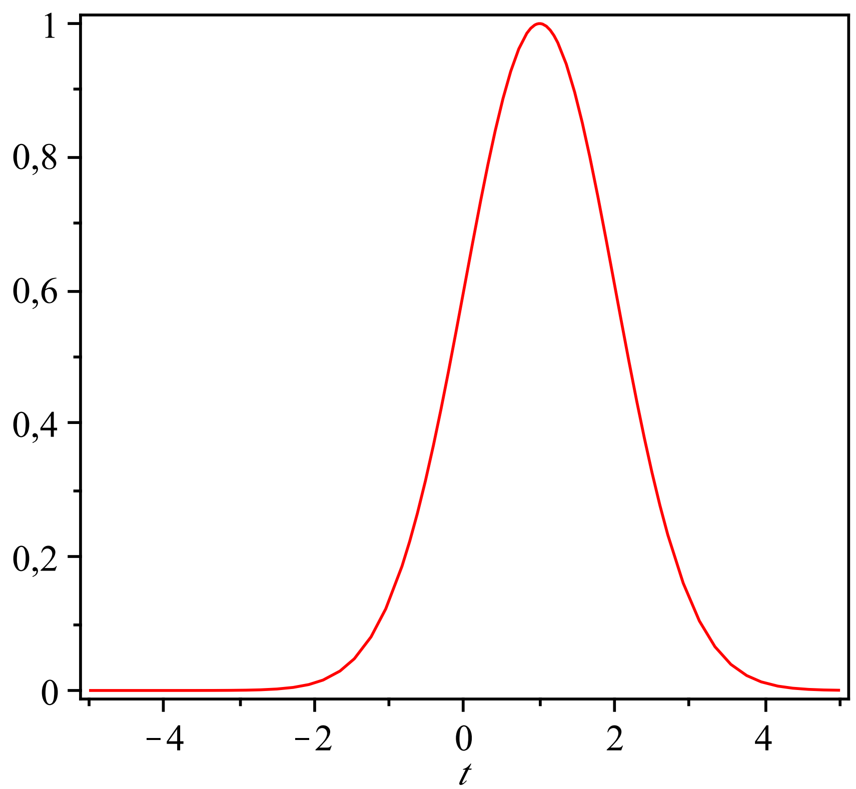

Reconstruction error

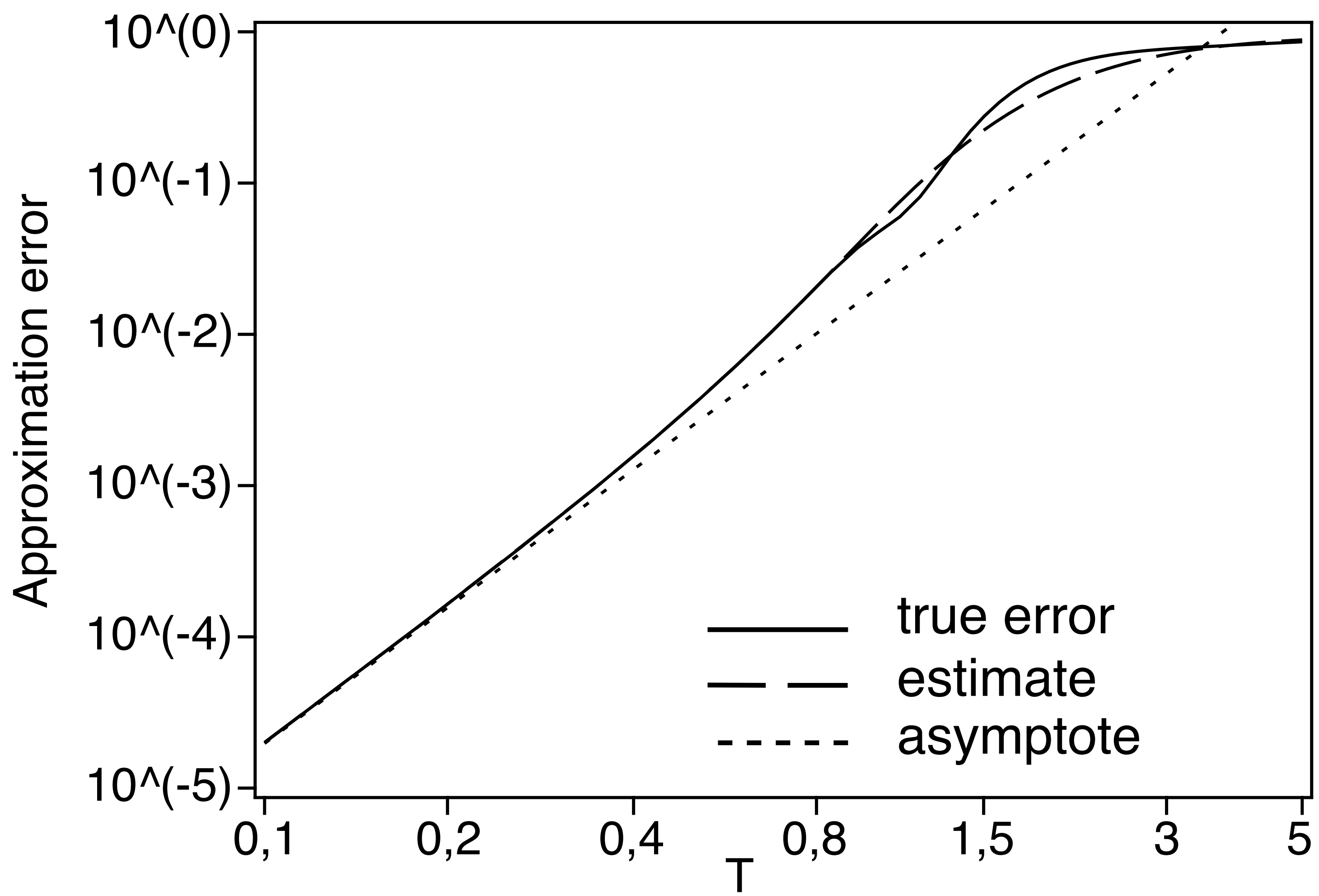

Error estimate: $\frac{1}{2\pi}\int_{\mathbb{R}} |\hat{s}(\omega)|^2 \omega^{2N} E(T\omega) d\omega$

Case study: reconstruction of the second derivative

- Method 1 : $\varphi = \beta^1 \qquad P(z) = z - 2 + z^{-1}$
  finite difference + linear spline interpolation
- Method 2 : $\varphi = \beta^3 \qquad P(z) = 6(z - 2 + z^{-1})/(z + 4 + z^{-1})$
  finite difference + cubic spline interpolation
- Method 3 : $\varphi = \beta^1 \qquad P(z) = 6(z - 2 + z^{-1})/(z + 4 + z^{-1})$
  second derivative of the cubic spline interpolant: $f_{\mathrm{der}} = f''_{\mathrm{app}}$
- Method 4 : $f_{\mathrm{der}}(t) = \frac{1}{\varepsilon^2}\Big(f_{\mathrm{app}}(t-\varepsilon) - 2f_{\mathrm{app}}(t) + f_{\mathrm{app}}(t+\varepsilon)\Big)$
  finite difference on the cubic spline interpolant f_{app}

Case study: reconstruction of the second derivative

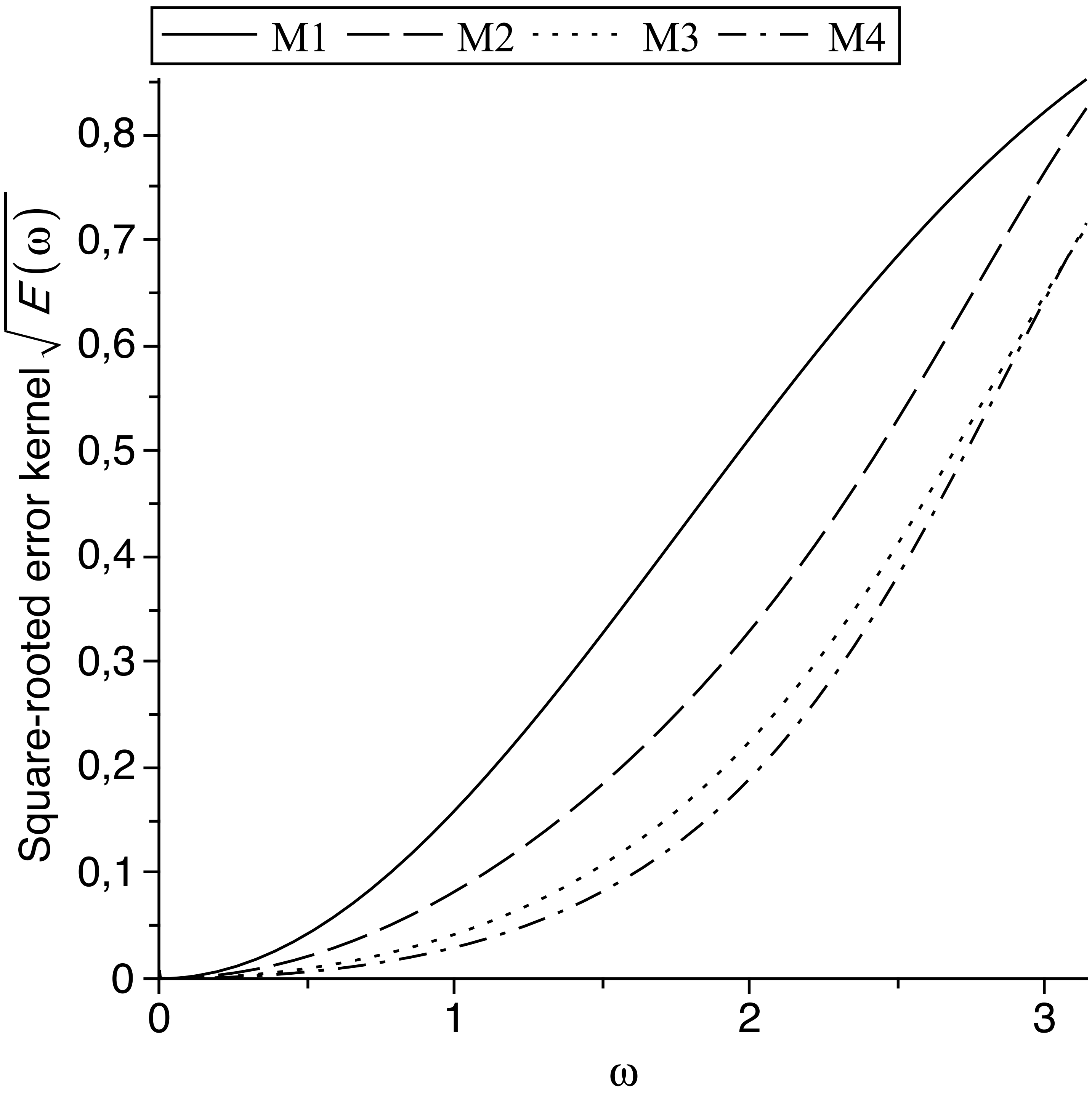

- M4 best with $\varepsilon \approx 0.43$
- All methods have approximation order 2
- M4 > M3 > M2 > M1

Case study: reconstruction of the second derivative

- Method 1 : $\varphi = \beta^1 \qquad P(z) = z - 2 + z^{-1}$
  finite difference + linear spline interpolation

- Method 2 : $\varphi = \beta^3 \qquad P(z) = 6(z - 2 + z^{-1})/(z + 4 + z^{-1})$
  → $L < L_\varphi = 4$: the prefilter is not optimal

- Method 3 : $\varphi = \beta^1 \qquad P(z) = 6(z - 2 + z^{-1})/(z + 4 + z^{-1})$
  → performs the orthogonal projection in $V_T(\beta^1)$

- Method 4 : $f_{\mathrm{der}}(t) = \dfrac{1}{\varepsilon^2}\Big(f_{\mathrm{app}}(t-\varepsilon) - 2f_{\mathrm{app}}(t) + f_{\mathrm{app}}(t+\varepsilon)\Big)$
  finite difference on the cubic spline interpolant f_{app}

Conclusion

- The frequency error kernel is a powerful tool to evaluate and design linear reconstruction methods
  - optimal quality for a given computation cost
- Possible extensions:
  - Noisy case
  - Gradient reconstruction on non-Cartesian lattices (e.g. BCC in 3D) with applications to visualization [Alim, Möller, Condat IEEE TVCG, 2010]
  - Applications to control theory